– Supplementary Information –

Electrical Breakdown of Multilayer MoS_2 Field-Effect Transistors with Thickness-Dependent Mobility

Rui Yang[1], Zenghui Wang[1], Philip X.-L. Feng[1,*]

[1]*Department of Electrical Engineering & Computer Science, Case School of Engineering*
Case Western Reserve University, 10900 Euclid Avenue, Cleveland, OH 44106, USA

1. Experimental Details of Electrical Breakdown Measurements

The multilayer MoS_2 devices experience multiple sweeping cycles in the electrical breakdown measurement (as shown in Fig. 4 in the Main Text). In the measurements, we start with smaller sweeping ranges for V_D, and then gradually increase the voltage range. We repeat multiple times for each V_D range and observe changes in device characteristics, including breakdown. Figure S1 shows the details of V_D sweeps. We observe in multiple devices (Figs. S1 (c)-(h)) that the current levels gradually decrease with subsequent sweeping cycles. Different breakdown locations on the devices are observed (Fig. S1 insets).

[*]Corresponding Author. Email: philip.feng@case.edu

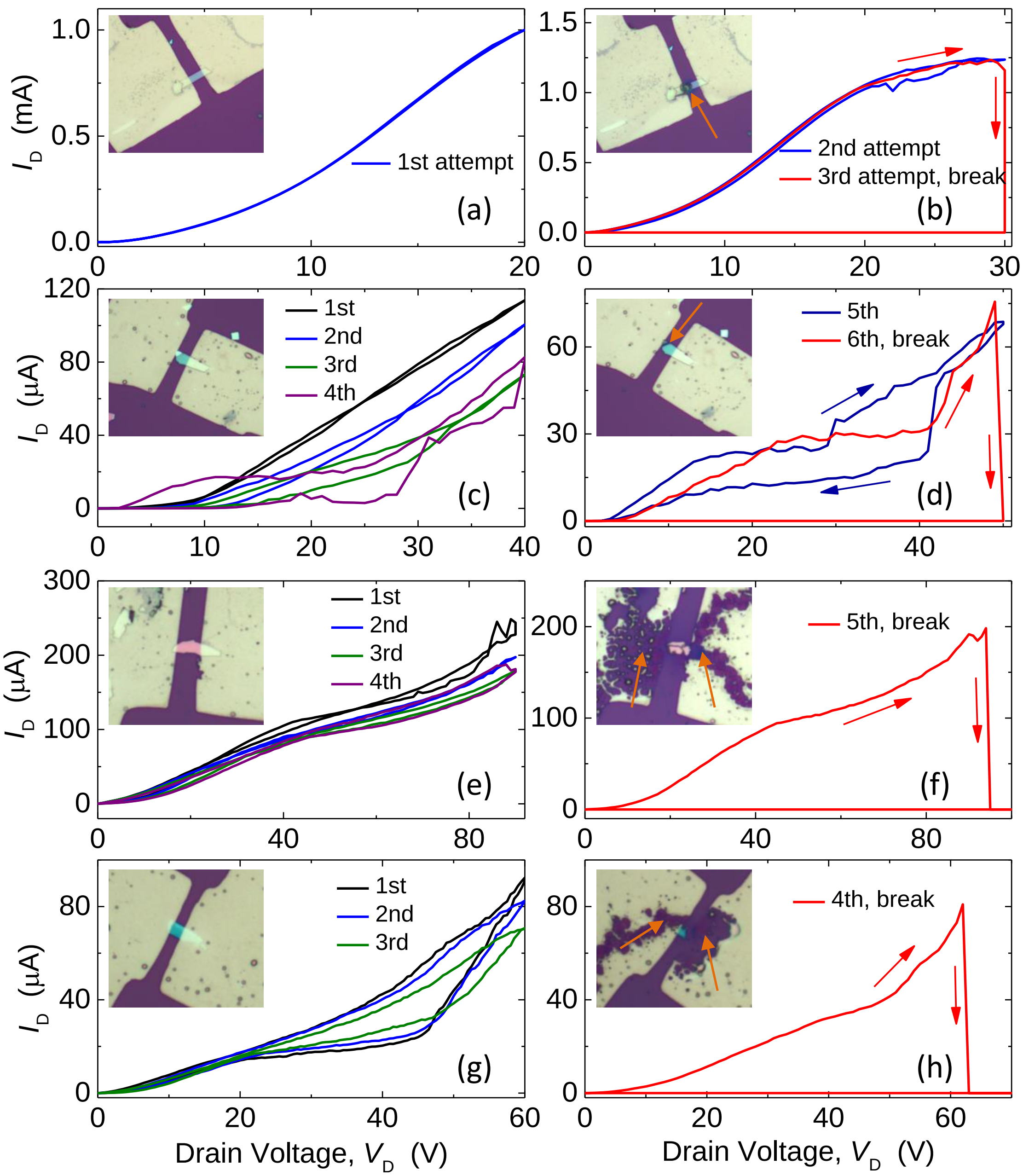

Fig. S1: V_D sweeps during the electrical breakdown measurement of multilayer MoS_2 transistors shown in Fig. 4 in the main text, with (a)-(b) for the device in Fig. 4(a), (c)-(d) for the device in Fig. 4(b), (e)-(f) for the device in Fig. 4(c), and (g)-(h) for the device in Fig. 4(d). The red curves show the final breakdown sweeps. Insets: Optical microscope images before (a,c,e,g) and after (b,d,f,h) the breakdown.

2. **Scattering Mechanisms**

We model the device mobility dependence on thickness with different scattering mechanisms, and the relaxation time for each scattering mechanism is plotted in Fig. S2 for MoS_2 thickness of 2.5nm to 86nm, which corresponds to 4 to 140 layers, using 0.615nm as the layer spacing[1]. As phonon scattering and charged impurity scattering in MoS_2 has been reported elsewhere[1,2,3,4,5], here we focus on other mechanisms, including boundary scattering (assuming the electron mean free path is on the order of MoS_2 thickness)[6], vacancy scattering (in calculation we use values of vacancy defect density n_v=10^{13}cm^{-2}, electron density n_e=10^{12}cm^{-2}, and vacancy radius comparable to the lattice constant)[7], and thickness step scattering (assuming average step distance of ~1.5μm, and step height comparable to the single layer thickness)[8]. We calculate these scattering mechanisms in MoS_2 and the results are shown in Fig. S2. The total relaxation time is calculated for different fitting parameters β (2, 4, and 6) as shown in the main text.

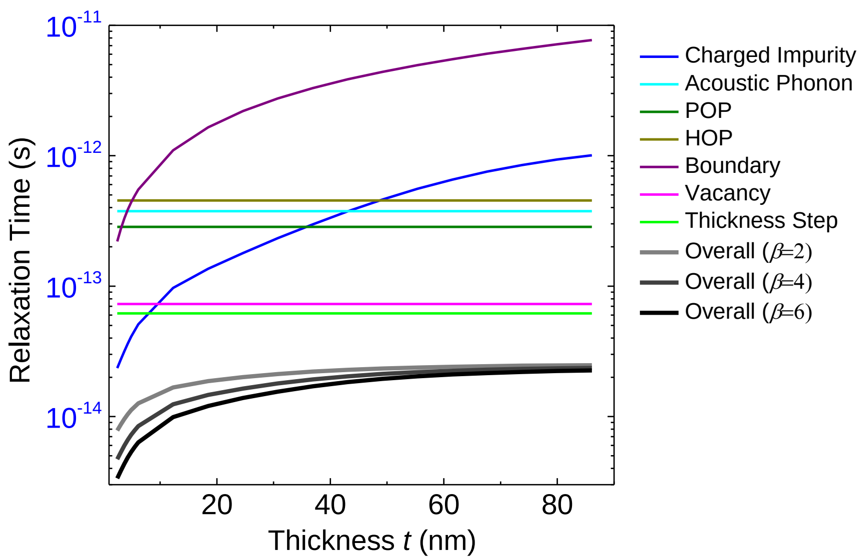

Fig. S2: Relaxation time for different scattering mechanisms with different MoS_2 thickness.

3. Details of FEM Simulation for Electrical Breakdown

In the electrical breakdown simulation (as shown in Fig. 6 in the Main Text), we use σ=35000S/m in Figs. 6(a)-(c)[9]. In the model we assume the MoS_2 extends 1μm into the contact, with 8kΩ contact resistance[10]. The heat is generated in MoS_2 channel and contact region and is dissipated to the SiO_2 and Si substrate, using thermal conductivity of SiO_2 and Si of 1.4W/(m K) and 130W/(m K), respectively. The surface of the substrate is held at room temperature (293.15K). The cross-section view of the FEM result (Fig. S3) shows that the heat dissipation into the substrate dominates.

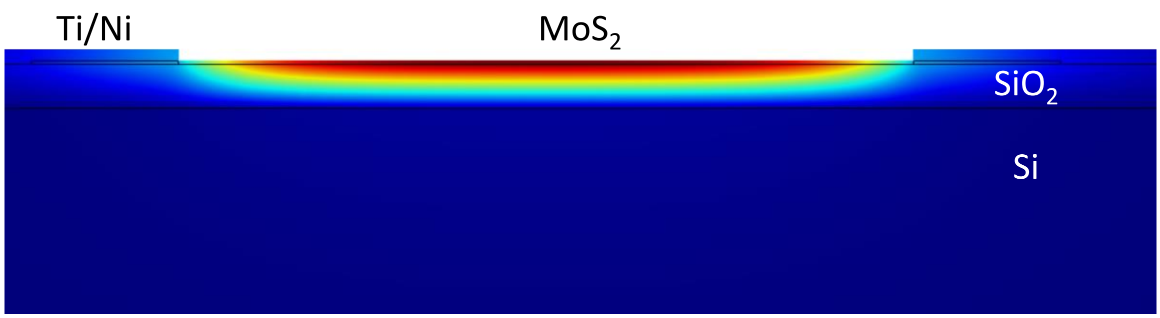

Fig. S3: The cross-section view of the FEM result of the temperature profile under Joule heating. In simulation the MoS_2 has t=25nm, L=5μm, W=2μm.

4. Summary of All the Measured Devices

Table S1: List of measured multilayer MoS_2 FETs and the parameters

Device ID #	MoS_2 Thickness (nm)	SiO_2 Substrate Thickness	Contact Materials	Mobility ($cm^2/(V\ s)$)	I_{On}/I_{Off} Ratio	Comments
1	70.3	290nm	Ti(3nm) /Ni(50nm)	42	10^4	Figs. 2(a)-2(d), Highest Mobility
2	5.7	290nm	Ti(2nm) /Ni(150nm)	9.9	4×10^6	Figs. 2(e)-2(h)
3	12	290nm	Ni(50nm)	18.3	6×10^4	Fig. 4(d)
4	18.4	290nm	Ti(2nm) /Ni(150nm)	6.5	10^6	
5	55	290nm	Ni(50nm)	38.7	7×10^4	Fig. 4(c)
6	76/22 Step	290nm	Ni(50nm)	2	6×10^4	Fig. 4(b)
7	32	290nm	Ti(5nm) /Ni(100nm)	36.8	10^7	Highest I_{On}/I_{Off} Ratio
8	12	290nm	Ti(5nm) /Ni(100nm)	9.8	10^6	
9	39	3.5µm	Ti(5nm) /Ni(150nm)	31.9	10^5	
10	7	3.5µm	Ti(5nm) /Ni(70nm)	1.6	10^3	

References

[1] S.-L. Li, K. Wakabayashi, Y. Xu, S. Nakaharai, K. Komatsu, W.-W. Li, Y.-F. Lin, A. Aparecido-Ferreira, K. Tsukagoshi, Nano Lett. **13**, 3546 (2013).

[2] N. Ma, D. Jena, Phys. Rev. X **4**, 011043 (2014).

[3] K. Kaasbjerg, K. S. Thygesen, K. W. Jacobsen, Phys. Rev. B **85**, 115317 (2012).

[4] B. L. Gelmont, M. Shur, M. Stroscio, J. Appl. Phys. **77**, 657 (1995).

[5] S. Kim, A. Konar, W.-S. Hwang, J. H. Lee, J. Lee, J. Yang, C. Jung, H. Kim, J.-B. Yoo, J.-Y. Choi, Y. W. Jin, S. Y. Lee, D. Jena, W. Choi, K. Kim, Nat. Commun. **3,** 1011 (2012).

[6] P. E. Hopkins, J. Appl. Phys. **105**, 093517 (2009).

[7] J.-H. Chen, W. G. Cullen, C. Jang, M. S. Fuhrer, E. D. Williams, Phys. Rev. Lett. **102**, 236805 (2009).

[8] Y. Tokura, T. Saku, Y. Horikoshi, Phys. Rev. B **53**, R10528 (1996).

[9] B. Radisavljevic, A. Kis, Nat. Mater. **12**, 815 (2013).

[10] B. W. H. Baugher, H. O. H. Churchill, Y. Yang, P. Jarillo-Herrero, Nano Lett. **13**, 4212 (2013).